Monatshefte für Chemie 131, 527–547 (2000)

Monatshefte für Chemie
Chemical Monthly

Invited Review

Modelling of Enzyme Properties in Organic Solvents

Giorgio Colombo, Gianluca Ottolina, and **Giacomo Carrea***

Istituto di Biocatalisi e Riconoscimento Molecolare CNR, I-20131 Milano, Italy

Summary. In this article we review how molecular modeling techniques can be used to shed some light on the influence of organic solvents on the molecular characteristics of proteins and enzymes. Molecular dynamic simulations on bovine pancreas trypsin inhibitor, chymotrypsin, and subtilisin make it possible to get a deeper understanding into how increased intramolecular interactions improve conformational rigidity, thus explaining the lower reactivity and the higher thermostability of enzymes in non-aqueous media. The application of thermodynamics-based models allows first qualitative predictions on the selectivity of many reaction types; however, the application of quantum mechanical/molecular mechanical methods is required for the development of quantitative models of actual reactivity patterns.

Keywords. Molecular modelling; Structure; Reactivity of enzymes; Organic solvents.

Introduction

The suspension or dissolution of enzymes in non-aqueous media affords many advantages (as well as some disadvantages) over the use of proteins in aqueous solution. For example, *Klibanov* and coworkers have demonstrated that proteins exhibit increased thermostability [1], molecular *pH* memory [2], and altered substrate specificity [3] when placed in an anhydrous organic solvent. Furthermore, the ability of enzymes to catalyze reactions that are either kinetically or thermodynamically impossible in water has also been observed [4–6]. This led to widespread use of enzymes as highly specific catalysts in non-aqueous solvents in the synthesis of organic compounds. For instance, a number of peptides containing *D*-amino acid residues have been synthesized using subtilisin as a catalyst, which is impossible in water because of the enzyme's strict *L*-stereoselectivity [7]. The synthetic potential of this phenomenon was also exploited in the subtilisin-catalyzed acylation of carbohydrates in anhydrous dimethylformamide. Not only does subtilisin esterify a number of sugars and related compounds in this solvent, but it does so on a preparative scale and with a marked positional selectivity [7]. Lipases and other hydrolases in non-aqueous

* Corresponding author

solvents also catalyze a variety of reactions like esterifications, transesterifications, aminolysis, and thio-transesterifications, whereas in water these processes are almost completely suppressed by hydrolysis [8].

The tyrosinase-catalyzed oxidation of phenols is another example. In water, this reaction proceeds with negligible yields due to the rapid polymerization of the resulting *ortho*-quinones and inactivation of the enzyme. In contrast, in chloroform, where both species are more stable, the quinones are readily obtained [9].

The possibility to apply biocatalysis to the synthesis of a wide range of compounds with high enantiomeric excesses as well as the new thermostability characteristics that enzymes can develop in organic solvents spurred investigation towards a deeper understanding of how protein structure and reactivity are affected by anhydrous organic solvents. The rationalization of these effects is supposed to enhance our ability to employ proteins as catalytic agents in non-aqueous media. This review will focus on different modelling approaches to the study of several properties of enzymes in these media. First, we will concentrate on enzyme structural properties in organic solvents, whereas in the second part the stress will be put on reactivity issues.

Protein Conformation in Organic Media

Flexibility and solvent accessible surface area

In addition to retaining catalytic activity, enzymes exhibit profound enhanced thermostability in organic solvents [10, 11]. Furthermore, it was found that in organic solutions it is possible to ''imprint'' the protein with an inhibitor and to induce changes in the enzymatic rate and selectivity after removal of the inhibitor [12, 13]. These characteristics of enzymes in organic solutions have been explained on the basis of increased rigidity of proteins in non-aqueous media. *Klibanov* and others have proposed that water acts as a ''molecular lubricant'', resulting in greater protein flexibility [14–17]. However, scant information is available at the molecular level to prove or to disprove this proposal. In order to accurately assess the role of flexibility in the activity of proteins, information concerning protein flexibility in both aqueous and nonaqueous environments was required [18].

Computer simulations have proven to be a valuable tool in the understanding of protein structure and dynamics [19, 20]. Since the seminal work of *McCammon*, *Gelin*, and *Karplus* demonstrating the dynamic nature of protein structures [19], numerous studies have appeared examining the behavior of proteins in the crystal lattice, *in vacuo*, and in aqueous solution [19]. These studies have shown that proteins possess a wealth of conformational substates of nearly equal energy [21]. The surrounding medium may influence protein flexibility by altering the energetic barriers separating these conformational substates and thereby affect the ease with which the protein may sample these states. *Hartsough* and *Merz* [18] provided one of the first molecular level pictures of a protein in a non-aqueous environment by simulating the behavior of bovine pancreatic trypsin inhibitor in water and chloroform *via* molecular dynamics calculations (MD). By this means the authors were able to evaluate the influence of the solvent upon protein structure and dynamics. After defining protein flexibility/rigidity of a protein as a measure of the

Table 1. Flexibility of BPTI (see Eq. 1) [18]

Run	$\langle RMS_{all} \rangle$/Å	$\langle RMS_{back} \rangle$/Å
H_2O, 298 K	0.741	0.531
$CHCl_3$, 298 K	0.528	0.418
$CHCl_3$, 310 K	0.614	0.476
$CHCl_3$, 360 K	0.630	0.512

amount by which instantaneous structures deviate from a time-averaged structure (Eq. (1)), the authors found that protein flexibility and solution temperature were intrinsically related.

$$flexibility = \langle (\langle (r_i - \langle r_{ave} \rangle)^2 \rangle)^{1/2} \rangle \quad (1)$$

Bovine pancreas trypsin inhibitor (BPTI) in water as the solvent was calculated to be more flexible than BPTI in chloroform solution, even when the temperature of the chloroform solution was 50°C higher than that of the aqueous solution. (Table 1). Examination of the differential flexibility of each residue revealed that the increased flexibility of BPTI in water was distributed over several residues of the protein, the increase being greater for the terminal residue. Switching from water to chloroform strongly influenced the conformations of the amino acid side chains. In water, the side chains of the surface residues were almost fully extended into the solvent, whereas in chloroform the side chains were found to be folded back onto the surface of the protein. Consistent with this findings were the differences in the amount of solvent accessible surface area: using a common probe of 1.4 Å to facilitate comparisons, the solvent accessible surface area of BPTI was 4300 $Å^2$ in water and 3700 $Å^2$ in chloroform. From this evidence, it is apparent that the organic medium is unable to stabilize polar/charged side chains; these are folded back into the enzyme, thus reducing surface area. This observation that side chains do not contact with the organic solvent anymore was used to rationalize the increased thermostability of the protein in non-aqueous medium. In order for a protein to unfold, various hydrogen bond and salt bridge contacts must be disrupted. The ability to form hydrogen bonds with the solvent is important for protein unfolding. This will not be possible in the organic environment. This observation offered a good explanation to the noted increase of protein stability in nonpolar solvents [1, 3, 10, 22].

Furthermore, these results offer a possible explanation for "molecular imprinting" [12]. If the active site of the enzyme involves polar/charged residues, these side chains would be unable to reorient significantly in the organic environment. Once moved to their correct position by the inhibitor/imprinter, the polar residues would be unable to return to their old positions, as this would involve exposing these groups to the nonpolar solvent. This study was one of the first to provide atomic-level insights into the picture of a protein in a nonpolar environment. It showed that placing a protein in a non-aqueous environment results in a significant loss of conformational flexibility and a significant change in the side-chain conformations upon moving from aqueous to non-aqueous environment.

In another study on BPTI [23], *Hartsough* and *Merz* presented a detailed analysis using a MD approach of the dynamics of both protein and solvent, and the results

Table 2. Radius of gyration and *SASA* for BPTI [23]

Simulation conditions	$\langle r_{gyr} \rangle$/Å	$SASA \times 10^3$/Å^2
$CHCl_3$, 300 K	10.88	3.64
$CHCl_3$, 310 K	10.90	3.65
H_2O, 310 K	11.50	4.18

were compared to corresponding simulations in water. The results clearly demonstrated the profound effect the solvent environment can exert on protein structure and dynamics. In a polar aqueous environment, protein-solvent interactions obviously can successfully compete with protein-protein interactions. This is primarily true because of the charge separation present in the water molecule. The large partial charges on the hydrogen atoms of water present the opportunity for large-magnitude electrostatic interactions with the protein. By contrast, there is much less charge separation in the chloroform molecule, and the advantageous protein-solvent interactions are of a smaller magnitude. Accordingly, in a nonaqueous environment the protein must look for other sources of electrostatic stabilization. In chloroform the primary source of electrostatic stabilization available to charged side chains are the chloride counterions and other functional groups on the surface of the protein. The reduced mobility of the chloride ions was indicative of how small the intensity of solvent-charge interaction is in the chloroform-protein system. In water, both chloride ions and protein can establish more favorable interactions with each other and with the solvent. The conversion of protein-solvent interactions into protein-protein interactions has a substantial effect on enzyme properties. When protein-solvent contacts are replaced by protein-protein contacts, the enzyme decreases in size and increases in stability (Table 2). It has been pointed out that the greater thermal stability can be attributed to the cross-linking effect of protein-protein interaction. Although not as intense as chemically bonded cross-links, the strength of the electrostatic interactions will be substantial. Moreover, some distortions in the protein structure were observed, as indicated by the different amount of solvent accessible surface area.

Hydrogen bond network

An increasing network of protein-protein interaction should reduce the ability of the protein to unfold or undergo hinging motions. Simulations provided evidence that such motions will be inhibited by non-aqueous solvents. These results are also supportive of the experimental findings of higher rigidity/thermostability in organic solvents. The consequences of this intricated cross-linking network of hydrogen bonds was manifested in several experimental observations.

Merz proposed to use the above principles of cross-linking and intramolecular networking to design enzymes of even greater stability in organic solvents: the creation of salt bridges will preferentially stabilize the folded state. Specifically, if a pair of nonpolar residues, which are distant in the primary sequence, yet spatially proximate in the native state, are mutated to a positive/negative ion pair, a substantial increase in the stability of the folded state will result. In the fully solvent-exposed

unfolded state, each of the charged residues will be relatively unstable in the nonpolar medium. Conversely, in the folded state an energetically favorable salt bridge will be formed by the ion pair. This new interaction will provide not only additional thermodynamic stability for the folded state but also an increased kinetic barrier to unfolding. This was also one of the first examples of an extensive use of MD simulations not only to study the behavior of enzymes in non-natural environments, but to provide insights and suggestions on how to improve protein molecules as catalysts.

In a recent paper, *Toba et al*. [24] have investigated the serine protease γ-chymotrypsin (γ-CT) in three different solvation environments using molecular dynamics. Unlike BPTI, γ-CT has been extensively used as a catalyst in several organic solvents for peptide synthesis and transesterifications [7], and the catalytic activities of serine protease have been well known for long. Moreover, the structure of the inhibited enzyme soaked in hexane as derived by X-ray diffraction was known [25, 26]. The simulations were: (1) γ-CT taken from the crystal structure of *Yennawar et al*. [25, 26] with seven surface bound hexane molecules and fifty essential water molecules all immersed in 1109 hexane molecules (simulation labeled CT); (2) γ-CT taken from Refs. [25, 26], solvated with fifty essential water molecules and immersed in 1107 hexane molecules (simulation CTWAT); and (3) γ-CT taken from Refs. [25, 26] solvated with a monolayer of 444 water molecules and immersed in 931 hexane molecules (simulation labeled CTMONO). From these trajectories the authors were able to find that the location of bound water molecules and the amount of hydration of the protein in the simulated structure had an effect on the protein flexibility as indicated by the changes in the root mean squared (*RMS*) deviation (Table 3). The radius of gyration value was similar for the three systems, indicating no significant unfolding or denaturation. Hydrophobic residues were found to have increased solvent accessible surface areas (*SASA*), whereas hydrophilic residues experienced a decrease in *SASA* in the CT and CTWAT simulations. No hexane diffusion into the interior of the protein was observed. Secondary structure analysis revealed that the active site structure was maintained in all simulations. Moreover, all fluctuations in positions and angles were within the scatter usually associated with protein fluctuations. This indicates that the active site of chymotrypsin remains relatively unchanged, which is in accordance with structural measurements of active enzymes in most organic solvents. The fluctuations in the simulation with water as the solvent were greater than those observed in the organic solvents. This observation corroborates the idea that proteins in non-aqueous solvents are less flexible; if the flexibility of the active site residues is critical for catalytic activity, this might partially explain the reduced activity of enzymes in organic solvents.

The simulations also confirmed previous findings that intramolecular forces such as hydrogen bonds and salt bridges were stronger in the CT and CTWAT simulations as shown by the increase in the number of stable hydrogen bonds. Net ion pair interactions and a reduced ratio of surface area to protein volume also contributed to the stability of the protein in hexane. The authors concluded that the stability of the protein in organic media is due to an increase in intramolecular stabilizing interactions such as hydrogen bonds, net ion pair interactions, and the reduced ratio of surface area to volume. The relatively hydrophobic protein interior

Table 3. Summary of the *RMS* deviation, radius of gyration, *SASA*, hydrophobic exposed *SASA*, and number of hydrogen bonds from the simulations on γ-chymotrypsin in three different solvation environments [24]

Analysis type	CT	CTWAT	CTMONO
	RMS deviation / Å		
Total	2.7	2.4	2.5
Backbone	2.4	2.1	2.0
	Radius of gyration / Å		
Minimized Structure	18.0	17.5	17.7
MD average	17.8	17.1	17.3
	SASA $\times 10^3$ / Å^2		
Crystal Structure	9.2	9.2	9.2
MD average	8.7	8.7	9.2
	Hydrophobic residues *SASA*/Total *SASA* (% exposed residues)		
Crystal Structure	34.8	34.3	34.3
MD Average	39.8	39.1	38.3
	Number of hydrogen bonds		
Crystal (total)	183	183	183
Min. Structure (total)	216	193	203
< 10%	216	224	294
> 90%	139	141	93

and the hydrophilic active site appear to be unaffected by the presence of the non-aqueous solvent.

In 1996, *Zheng* and *Ornstein* reported an MD simulation study of subtilisin Carlsberg in *DMSO* [27]. They compared their results to previous simulations carried out for water, acetonitrile, and carbon tetrachloride [28, 29]. *DMSO* is a dipolar, aprotic solvent with a dielectric constant of 46.5. It can compete with protein hydrogen bond acceptors for hydrogen bond donors. This is similar to acetonitrile, but *DMSO* is a much better hydrogen bond acceptor and, therefore, one of the few protein-dissolving solvents; and it has been used widely as an alternative solvent to water, due to the high solubility of peptides and proteins in it. *Zengh* and *Ornstein* also used quantum mechanics calculations to examine the hydrogen bonding interactions between *DMSO* and water and between *DMSO* and an amide hydrogen, using formamide as a model for the amide.

After analysis of their 745 ps trajectory they found that the structure of the protein was still not very different from the crystal structure in aqueous medium. However, some major differences could be noticed for DMSO, compared to other solvents. During the simulation for *DMSO*, the five residues of the N-terminus moved away and lost contact with the rest of the protein. This was in accordance with previous findings that *DMSO* is a protein denaturing medium. NMR studies by *Desai* and *Klibanov* also suggested that *DMSO* can cause partial unfolding of BPTI [30]. In addition, the simulation showed that *DMSO* was capable of stripping water

molecules away from the protein surface, a phenomenon related to the hydrophilicity of the solvent. More water molecules were seen to leave the protein in *DMSO* than in acetonitrile, whereas in a hydrophobic solvent such as CCl_4 no water left the protein surface during the simulation. This was also in agreement with experimental observations [30]. It is worth noting that *DMSO* was found to be able to sequester a metal ion from the protein and coordinate it. The ability of polar solvents to sequester metal ions seems to be supported by the observation that when subtilisin crystals grown in water were soaked in acetonitrile, two metal ions were lost. This important observation provided an explanation to previous reports on the role of salts on protein stability and activity in organic solvents. The presence of salt ions can prevent direct contacts between organic solvents and the protein either by retaining more water molecules during lyophilization or by coordinating to solvent molecules to form complexes.

In these simulations [27–29] *Zheng* and *Ornstein* also found that the calculated number of intra-protein hydrogen bonds are different in *DMSO*, acetonitrile, and CCl_4 compared to water. The calculated average numbers of intra-protein hydrogen bonds were 247 ± 6, 259 ± 7, 264 ± 7, and 214 ± 7. Thus, the general trend that there are more intra-protein hydrogen bonds for a protein in a nonaqueous environment than in water seems to be followed once again. Through the application of quantum mechanics, the hydrogen bonding between *DMSO* and water was found to be stronger than the hydrogen bond between two water molecules, which was in agreement with experiment [27]. The calculations also showed that hydrogen bonding between *DMSO* and an amide hydrogen is stronger than between a carbonyl oxygen and an amide hydrogen [27], thus providing a good explanation why *DMSO* is a protein-dissolving solvent and is capable of inducing unfolding or deactivation of the enzyme.

Ornstein [31] also examined the effect of solvent environments on protein salt bridges by performing high level *ab initio* molecular orbital calculations in the gas phase and in three different solvents on a model compound represented by formate and guanidinium ions (Fig. 1). The energy difference between the neutral hydrogen-bonded complex and the zwitterionic form as well as the interconversion barrier between them was investigated in detail at 6-31G*, 6-311+G**, MP2/6-31G*, and MP2/6-311+G** levels. For calculations in solutions, the *Onsager* solvent reaction field model was used [32]. Three solvents (H_2O, *DMSO*, CCl_4) with different dielectric constants (78.3, 46.45, 2.238) were considered. In the gas phase, the neutral conventional hydrogen-bonded complex is predicted to be favoured at all four levels of theory. In a nonpolar, hydrophobic solvent like CCl_4, the energy difference between these two forms is small and the barrier that

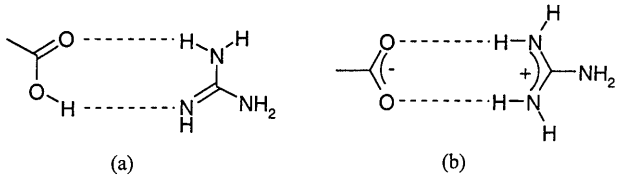

Fig. 1. Formate and guanidinium ion salt bridge: (a) neutral complex, (b) zwitterionic form [31]

Table 4. Calculated energy difference between the two forms of hydrogen-bonded complexes of formate and guanidinium (Figs. 1a and 1b) and the corresponding interconversion barriers [31]

Theory	Phase	Energy difference / $kJ \cdot mol^{-1}$	Forward barrier / $kJ \cdot mol^{-1}$
6-31 G	gas	22.6	33.1
6-311+G	gas	23.0	31.4
MP2/6-31 G	gas	14.2	16.3
MP2/6-311+G	gas	20.1	14.6
6-31 G	CCl_4	−0.4	22.6
6-311+G	CCl_4	0.8	20.9
MP2/6-31 G	CCl_4	−0.8	6.3
MP2/6-311+G	CCl_4	4.2	5.4
6-31 G	*DMSO*	−36.8	10.9
6-311+G	*DMSO*	−37.7	8.4
MP2/6-31 G	*DMSO*	−21.3	0
MP2/6-311+G	*DMSO*	−25.5	0
6-31 G	H_2O	−38.1	10.5
6-311+G	H_2O	−38.9	8.4
MP2/6-31 G	H_2O	−22.2	0
MP2/6-311+G	H_2O	−26.4	0

separates them is also low, but the neutral conventional hydrogen-bonded complex still seems to be slightly favoured. However, in polar solvents like *DMSO* and water, the zwitterionic form dominates (Table 4).

Ionized hydrogen bonds are often designated as salt bridges (or ion pairs) in crystallographic structures of proteins. In most cases, it is unknown on which atom the proton resides since X-ray crystallography cannot locate hydrogen atoms directly. In environments of low dielectric constant such as in non-aqueous solvents, membranes, and the interior of proteins, it is possible that the zwitterionic form will convert to the neutral hydrogen-bonded form *via* a proton shifting: calculations suggested that this really occurs in a very low dielectric environment [31]. Since a protein is not a homogeneous system with the same dielectric constant throughout, the microenvironment for each salt bridge could be different. Normally, salt bridges are also hydrogen-bonded to other polar groups or nearby water [33]; thus, the microenvironment for each salt bridge could be rather polar, and the effective dielectric constant could be larger than normally expected in the interior of a protein which is assumed to have a dielectric constant of 2–4 in most electrostatic models. Therefore, some of the interior salt bridges may still have significant zwitterionic character.

As seen before, MD simulations of proteins in non-aqueous solvents have shown that additional intra-protein hydrogen bonds and salt bridges are formed when a protein is transferred from an aqueous to a non-aqueous environment. Based on their calculations, *Zheng* and *Ornstein* [31] believe that a salt bridge is in the zwitterionic form in a relatively polar microenvironment. In a non-polar environment with very small dielectric constant it will probably prevail in the neutral form. Ref. [31] offers once more the suggestion that for a protein to have

optimal activity in a nonpolar solvent isolated charged groups must be removed (by site-directed mutagenesis) in order to increase its stability. However, if a charged group has an oppositely charged group nearby to which it could form a salt bridge either in aqueous or in non aqueous solution, the interconversion between the neutral and zwitterionic forms *via* proton transfer is an effective way to annihilate charge separation.

Summarizing, by means of MD simulations several explanations can be given as to why enzymes have different structural characteristics in organic solvents compared to water: from all simulations a higher degree of intramolecular hydrogen bonding, improved salt bridge type interactions, and reduction of the surface area to volume ratio can be noticed in proteins and enzymes when soaked in organic solvents. All these factors contribute to the stability of the enzyme by preventing its possible unfolding through improving its intramolecular interactions. In addition, once unraveled, the amino acid side chains will experience less favorable contacts with the organic solvent which cannot hydrogen bond or electrostatically stabilize charged and polar side chains. Thus, the formation of the unfolded state can be considered to be more disfavoured in organic solvents than in water.

The higher number of intramolecular contacts can also be considered an important factor in determining the lower activity of enzymes in non-aqueous media: if the enzyme is, in fact, more rigid due to intraprotein interactions, it will be less able to adapt to the substrates entering the active site pocket. This phenomenon may be important as an explanation of the peculiar reactivity in organic solvents.

Modelling Enzyme Activity and Selectivity in Organic Media

A complete understanding of the enzyme-substrate-solvent interaction is necessary to increase enzyme utility to synthetic organic chemists [34, 35]. Several theories have been proposed to rationalize the mechanism by which organic media can influence reactivity.

In some cases, diffusional limitations have been claimed as the main cause of different and limited reactivity of enzymes in organic solvents. However, this possibility was ruled out by *Klibanov* and coworkers who have shown experimentally that slower catalysis is not due to mass transfer limitations [34].

Another hypothesis pointed out the change in conformation of the enzyme as the main cause of different reactivity compared to water. X-Ray crystallography experiments on crosslinked crystals of subtilisin soaked in both acetonitrile and dioxane showed that the three-dimensional structures of these proteins were virtually identical to their counterparts in water [36, 37]. Moreover, *Yennawar et al.* showed that uncrosslinked chymotrypsin in hexane had the same structure as in water [25]. By means of FT-IR spectroscopy, *Klibanov* and coworkers demonstrated that placing lyophilized subtilisin in organic solvents such as octane, acetonitrile, and dioxane had no appreciable effect on its secondary structure as indicated by its α-helix content [38].

The attention and the efforts of many researchers were then attracted to the study of the energy of binding between enzyme and substrate or to the study of the reaction intermediate (transition state) in the presence of both enzyme and solvent.

Thermodynamic approach and UNIFAC

A model proposed by *Klibanov* suggested that the selectivity dependence arises due to the differences in the thermodynamics of substrate solvation. Because this model has its basis in thermodynamics, it could make some quantitative predictions. One of the first applications involved the study of the substrate specificity of subtilisin Carlsberg in the transesterification reaction of N-Ac-*L-Ser*-OEt and N-Ac-*L-Phe*-OEt with 1-propanol in twenty different anhydrous solvents (Fig. 2). The serine substrate was strongly preferred in some solvents, whereas phenylalanine was preferred in others. The thermodynamic model represented specificity as a function of the solvent-to-water partition coefficients of the substrates and the substrate specificity of the enzyme-catalyzed hydrolysis of esters in water (Eq. (2)) [39].

$$\log((k_{\text{cat}}/K_{\text{M}})_{Ser}/(k_{\text{cat}}/K_{\text{M}})_{Phe})_{\text{solvent}} = \log(P_{Phe}/P_{Ser}) + \log((k_{\text{cat}}/K_{\text{M}})_{Ser}/(k_{\text{cat}}/K_{\text{M}})_{Phe})_{\text{water}} \quad (2)$$

Equation (2) predicts that a double-logarithmic plot of substrate specificity in any solvent *vs.* the P ratio will yield a straight line with a slope of 1, whose intercept with the ordinate should equal the substrate specificity in water. This model, while mechanistic and predictive, is essentially independent of the enzyme because the contribution of subtilisin-substrate binding is accounted for by the substrate specificity in water. Thus, this model should be applicable to any enzyme/substrate pair as long as the substrates are inaccessible to the solvent in the transition state.

However, a fundamental limitation of this approach is that it can be used only with water-immiscible solvents, because direct measurements of partition coefficients between water and water-miscible solvents are not feasible. In a second paper in 1993 those problems were overcome by introducing Eq. (3) [40] where γ is the thermodynamic activity coefficient of the substrate indicated.

$$P_{Phe}/P_{Ser} = (\gamma_{Ser}/\gamma_{Phe})_{\text{solvent}}/(\gamma_{Phe}/\gamma_{Ser})_{\text{water}} \quad (3)$$

The γ values for a given molecule in a solvent can be calculated on the basis of the *van der Waals* volumes and surface areas of the constituent groups of that molecule and of those of the solvent and from empirically determined interaction parameters

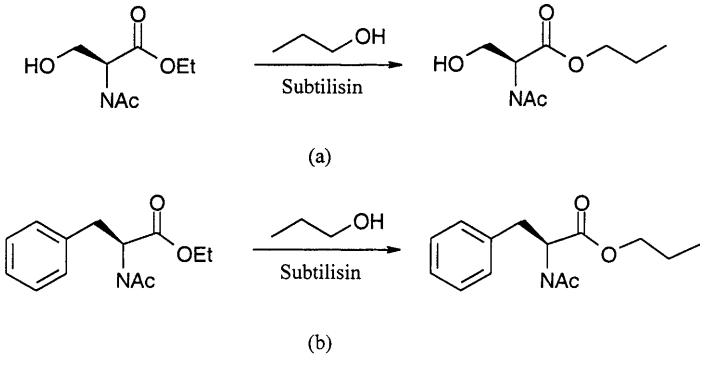

Fig. 2. Subtilisin-catalyzed transesterifications of N-Ac-*L-Ser*-OEt (a) and N-Ac-*L-Phe*-OEt (b) [39]

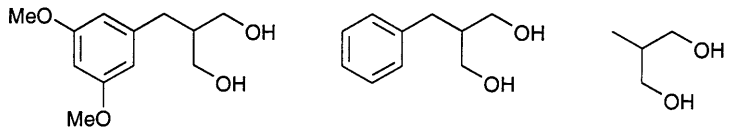

Fig. 3. 2-Substituted 1,3-propanediols [42]

between these groups. Such calculations can be carried out using the UNIFAC algorithm [41]. According to Eqs. (2) and (3) a double-logarithmic plot of substrate specificity *vs. P* ratios in several solvents should give a straight line as stated before. The authors were able to find a correlation coefficient of 0.96 for a line with a slope of 0.89 and an intercept of -1.7 (this was same as the experimental value of the log of the substrate specificity in water). Once again, the assumption that substrates be fully removed from the solvent in the transition state is made, which cannot be always true. Thus, *Klibanov* and coworkers devised a new thermodynamic method to rationalize the solvent dependence of any type of enzymatic selectivity (prochiral, diastereo-, or enantioselectivity) solely on the basis of the thermodynamics of substrate solvation [42]. The model predicts that selectivity (defined as the ratio k_{cat}/K_M) should be proportional to the ratio of the thermodynamic activity coefficients of the desolvated portions of the substrates in the relevant transition state of the enzymatic reaction. This ratio is calculated by a three step procedure: (*a*) determine the desolvated portion of the substrate in the transition state using molecular modeling based on the crystal structure of the enzyme, (*b*) approximate the desolvated portion of the substrate by a distinct model compound, and (*c*) calculate the activity coefficients of this model compound using the UNIFAC algorithm.

In the first study [42] the model was applied to the determination of the prochiral selectivity of enzymes, in particular γ-chymotrypsin and subtilisin Carlsberg used as asymmetric catalysts in the acetylation of 2-substituted 1,3-propanediols (Fig. 3). The relation on which the method is based is represented by Eq. (4).

$$\log((k_{cat}/K_M)_I/(k_{cat}/K_M)_{II})A = \log(\gamma_I/\gamma_{II}) + \log((k_{cat}/K_M)_I/(k_{cat}/K_M)_{II})B \quad (4)$$

In Eq. (4), I and II represent either the two transition state models for prochiral selectivity or for enantioselectivity. Moreover, if solvent B is fixed as a reference solvent, the final term in Eq. (4) can be taken as a constant, and the equation will assume the simplified form of Eq. (5).

$$\log((k_{cat}/K_M)_I/(k_{cat}/K_M)_{II})_A = \log(\gamma_I/\gamma_{II}) + const \quad (5)$$

From a theoretical point of view, the authors demonstrated that the selectivity depends only on the differences in the desolvation of the transition state. This is the point where molecular modelling comes into play: MD is, in fact, used to determine the desolvated portions of the two substrates leading to two different products. In the case of prochiral selectivity, very good results were obtained in the case of cross-linked crystal enzyme, where a correlation factor of 0.94 and a slope of 1 for the double-logarithmic plot of Eq. (5) was obtained.

Very good regression coefficients (∼0.93) were also obtained in the case of the enantioselectivity in the transesterification reaction of methyl 3-hydroxy-2-phenylpropionate in different organic solvents [43]. In this paper, however, the authors pointed out how the approximation of the desolvated part of the substrate can be made using different ''UNIFAC groups''. Moreover, it was shown that the predictivity degree of the method was heavily dependent on the choice of these approximating groups.

A Monte Carlo/Energy Minimization scheme was also used to determine the desolvated part of the transition intermediate model, and then the UNIFAC procedure was applied [44]. In this case, the UNIFAC approach proved to be able to give qualitative predictions, as well, but was unable to afford good quantitative correspondence between experimental and calculated values. *Luque et al*. applied this approach to the study of the role of transition state desolvation on enzymatic enantioselectivity in aqueous-organic mixtures using lipases as catalysts. The purely thermodynamic treatment resulted in very poor predictions of enantioselectivity [45]. A thorough analysis revealed that the energetics of substrate desolvation did not contribute significantly to the experimentally observed changes in the enantioselectivity of lipases. Therefore, other factors such as conformational changes in enzyme molecules induced by the solvents or differential solvent displacement from the active center of the enzyme by the substrate were claimed to be fundamental [45]. Thus, a more in-depth computational study was required to evaluate the influence of the solvent on enzyme reactivity, based on force-field or higher level studies of the interactions between the substrate, the enzyme, and, possibly, the solvent.

Transition state and molecular dynamics

Hult and coworkers [46] used information from the crystal structures of the *Candida antarctica* lipase type B (CALB; incubated with the detergent Tween 80, or inhibited by a racemic mixture of *n*-hexylchlorophosphonate ethyl ester) to model the tetrahedral intermediates of two acyl transfer reactions into the active site in order to explain the high selectivity of CALB towards certain secondary alcohols. The mechanism was assumed to be identical to the general one of serine-proteases or hydrolases. The first intermediate model represented the transesterification reaction of 1-phenylethanol with an octanoate ester as acyl donor. In the second intermediate, the hydrolysis of a glycerol butanoate derivative was studied (Figs. 4 and 5). Molecular dynamics and minimization techniques were used throughout. Starting models of the enzyme-substrate transition states were built as tetrahedral covalent complexes with the Oγ atom of the active site serine residue connected to the carbonyl carbon atom of the substrate. A protonated histidine residue in the catalytic triad was assumed to be present in the transition state. In this reaction mechanism, the protonated active site histidine forms hydrogen bonds to the Oγ atom of the catalytic serine and to the oxygen of the alcohol group of the substrate. Furthermore, the oxyanion of the transition state was forced to interact with the oxyanion hole residues. The energies and structures of the complexes were calculated by a combined energy minimization and molecular dynamics protocol [46]. Energy minima of the complexes were found by MD simulations *in vacuo* in

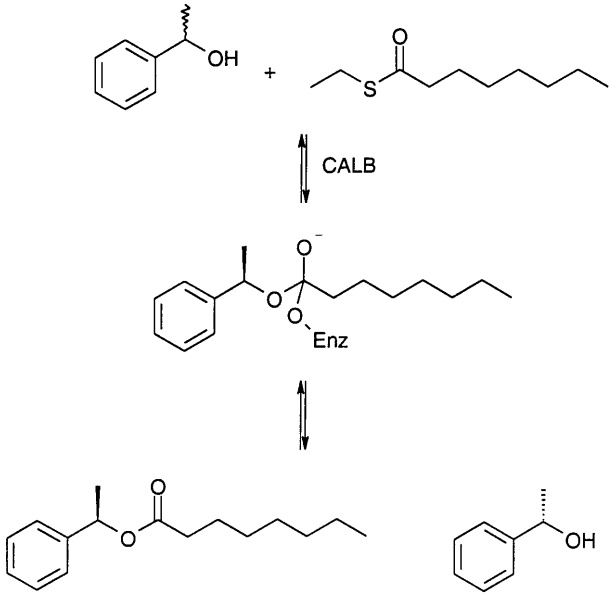

Fig. 4. Stereoselective resolution of 1-phenylethanol with CALB and thioethyl-octanoate [46]

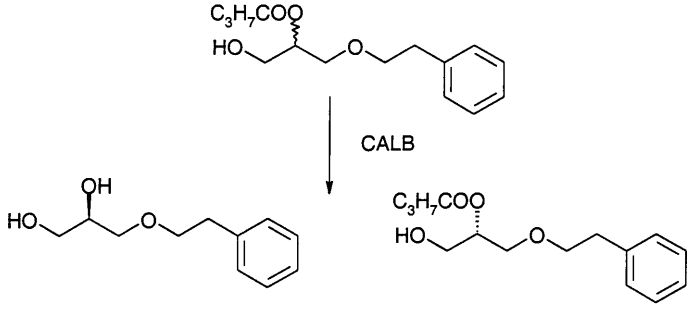

Fig. 5. CALB catalyzed stereoselective hydrolysis of glycerol butanoate derivative [46]

which the molecules were repeatedly heated to 300 K and slowly cooled to 1 K. The trapped conformations were then further minimized with 500 steps of energy minimization.

In the case of 1-phenylethanol the (*S*)-alcohol was found in such a conformation that it could not easily donate a proton to the catalytic hystidine 224 residue, which is considered to be essential for nucleophilic attack on the acyl enzyme. Consequently, in a hydrolysis reaction, the alcohol moiety of the substrate would be stuck in a position where it cannot accept a proton from the histidine and is therefore not efficient as a leaving group. On the other hand, the energy minima of the tetrahedral intermediate of the (*R*)-enantiomer contain a favourable hydrogen bond between the catalytic histidine and the oxygen atom of the alcohol group which would enable rapid proton transfer for catalysis.

In the glycerol derivative hydrolysis study, the fast reacting (*R*)-enantiomer was found to have all its bonds in the carbon chain of the large group in the relaxed *trans* conformations. The small group was interacting with *Trp*104 in the small pocket. On the other hand, the slow reacting (*S*)-enantiomer had its large group twisted away from the specificity pocket, in contact with the side chains of *Leu*278, *Ala*282, and *Ile*285 side chains. The presence of these side chains forced the carbon chain of this group of the substrate to adopt an energetically less favorable conformation. It was hypothesized that the enantiopreference for the (*R*)-enantiomer in the hydrolysis of glycerol butanoate was due to these strain differences in the substrate conformations. The results of this study (together with X-ray data) provided structural explanations for the high stereoselectivity of CALB toward secondary alcohols which can be extended to more general cases. However, all MD and energy minimization calculations presented in Ref. [46] were run *in vacuo* and gave only structural-sterical information about interactions between the enzyme and the tetrahedral intermediate.

Semiempirical and ab initio calculations

Haeffner et al. also proposed an MD-based molecular modelling method to predict the enantioselectivity in lipase-catalyzed transesterification reactions of the substrates of Fig. 6 [47]. A tetrahedral intermediate with a rigid central part was used to mimic the transition state. The geometric parameters were calculated by means of *ab initio* methods on the tetrahedral intermediate formed in the gas phase reaction between methyl acetate and a methoxide ion using the 6-31 + G^* basis set. The charges were calculated with an electrostatic potential (ESP) fitting methodology on the tetrahedral intermediate using 6-31 + G^* on RHF/STO-3G optimized geometry. The same set of charges was used for both enantiomers in all the three cases. After MD conformational steps and energy refinement of the obtained structures, enantioselectivity was expressed as a function of the energy differences between the two diastereoisomeric enzyme-substrate complexes. This energy difference evaluation was performed by defining subsets within the enzyme structures. Two different strategies were used. The first one used predefined parts of the enzyme and the substrate as subsets, whereas the second approach formed energy based subsets. The selection of the residues to be included was based on the energy of interaction between the specific residue and the transition state analogue. Importantly, this approach was able to predict which enantiomer was the fast-reacting one.

However, the issue of solvent influence, along with that of the electrostatic influence of the enzyme on reactivity, was not examined. This problem could be tackled by the use of mixed quantum mechanics/molecular mechanics (QM/MM) methods which were first introduced by *Warshel* and *Lewitt* [48]. Using this

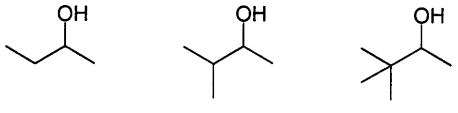

Fig. 6. Substrates used in the subsetting scheme devised by *Haeffner et al*. [47]

approach, the reactive events can be described at a QM level for the active site, whereas the rest of the protein is treated by MM or MD calculations. The two regions can interact through an interaction Hamiltonian; in this way, the active site (*i.e*. the QM region) can respond to the influence of its protein and solvent environment in terms of polarization, electron correlation, and charge transfer effects.

In 1991 *Kollman* and coworkers described semiempirical molecular orbital calculations of the serine protease catalyzed hydrolysis of amides and esters and the effect of the protein environment and dynamics on the process [49]. They found that the PM3 Hamiltonian was much better suited than the AM1 one at reproducing hydrogen bond geometries, and so the former was used to describe the reaction mechanism. The lowest energy pathway for formation of the tetrahedral intermediate was for serine to approach the substrate, followed by coupled heavy atom motion and proton transfer to complete the reaction. The importance of active site residues and the environment in stabilizing the substrate was addressed by evaluating particular interactions in fully solvated enzyme-substrate models. These interaction energies were calculated for both a noncovalent enzyme-substrate complex and a model for the tetrahedral intermediate in which a covalent bond was formed between the serine and substrate. The oxyanion hole and *Asp* greatly stabilized the active site region of the tetrahedral intermediate and, presumably, the transition state structure. The environment itself, excluding the active site residues and the oxyanion hole, was important in stabilizing the scissile bond of the substrate in the tetrahedral intermediate *vs.* the *Michaelis* complex. This was certainly one of the first important reports of the use of information gained from quantum mechanical simulations in elucidating mechanistic pathways in which the role of the protein environment was not negligible.

QM/MM approaches were used successfully to describe the structural and reactivity characteristics of metal containing enzymes, to design a charge model to describe the active site of these enzymes, and, finally, to describe the binding preferences of inhibitors to Zn(II) containing proteins [50].

Williams and coworkers were able to describe and characterize the transition structure for the reduction of pyruvate, catalyzed by lactate dehydrogenase (LDH), by means of QM/MM calculations involving a fully flexible active region comprising 1900 atoms and 5700 degrees of freedom [51].

Another successful application of this technique is due to *Antonczack et al*. who described the thermolysin catalyzed hydrolysis of formamide [52]. The first step of the reaction was proven to be the nucleophilic attack of the carbon atom by the oxygen of the water molecule or by a water dimer. The mechanism involving an ancillary water molecule is always favoured compared to the process in which a single water molecule is involved. The fact was explained by a better nucleophilicity of the oxygen atom in the water dimer. The zinc atom of the catalytic center acts as a *Lewis* acid and the ligands as electron reservoirs. To reach these conclusions, the authors needed an accurate description of the active site of the enzyme, taking into account the metal and the environment. In particular, the ligands of Zn(II) were seen to play an important role in delocalizing the charges along the reaction pathway. Thus, this study was feasible thanks to the possibility of describing the active site region at a good semiempirical level (AM1) and the rest of the molecule through a classical force field.

A striking application of this methodology to describe enzyme reactivity is due to *Warshel*'s group [53]. They developped an effective approach for *ab initio* calculations of activation energies in enzymatic reactions. Their approach used an empirical valence bond (EVB) potential surface as a reference potential for evaluating the free energy of a hybrid *ab initio* QM/MM potential surface. This procedure involved an automated calibration of the EVB potential using gas-phase *ab initio* calculations. The method was used to study the nucleophilic attack step in the catalytic reaction of subtilisin. It was found that the use of the EVB potential as a reference allowed the determination of the actual activation free energy of enzymatic reactions [53].

Amide hydrolysis in trypsin and water solution was studied by *Stanton et al.* [54]. They proposed a new more general method to combine *ab initio* quantum mechanical calculations with the classical mechanical free energy perturbation approach to calculate the energetics of enzyme-catalyzed reactions and the same reactions in solution. This method, enabling enzyme and solution reactions to be compared without the use of empirical parameters, was applied to the formation of the tetrahedral intermediate in trypsin. Two critical aspects of this new approach were: (*a*) the calculation of the reaction energetics in solution and (*b*) the use of the restrained electrostatic potential (RESP) protocol [55] to calculate the charge distributions of structures along the reaction pathway. This enabled the authors to circumvent the problem of partitioning the charge across a residue divided into QM and MM parts. These charges were then used along with standard parameters to define the force field representations of the complex in the free energy perturbation (FEP) calculations. Two sets of calculations were performed to obtain the differences in free energy between points on the reaction pathway. In the first set, the QM region was held static during the entire length of the simulation. In the second set of simulations, internal degrees of freedom of the QM region were allowed to relax in order to respond to the dynamics of the enzyme. In this way, the impact of active site flexibility on free energy calculations could be assessed. This protocol allows to examine the nature of enzyme catalysis by performing analogous simulations in water. Comparison of these two simulations yields insights into the role of the enzyme as a catalyst. The method is thus certainly general and applicable to the investigation of the energetics of enzyme reaction pathways.

Continuum and explicit solvents

The use of *ab initio* calculated charges to describe enantioselectivity was described by *Ke*, *Tidor*, and *Klibanov* [56]. The transition states for the acylation and deacylation of chymotrypsin by substrates **1**–**4** Fig. 7 were approximated by the corresponding transition intermediates. The substrate charge distribution for the (*R*) and (*S*) configured substrates was determined *via* STO-3G electrostatic potential fits using an ensemble of ten energy-minimized structures obtained from gas-phase MD simulations. The substrates were then docked into the enzyme active site, and vacuum (modelled using a distance-dependent dielectric) MD simulations followed by energy minimization were used to obtain suitable structures of the enzyme/substrate complexes. To mimic the presence of water, the authors used continuum electrostatic models, and the $\Delta\Delta G'$ activation energy

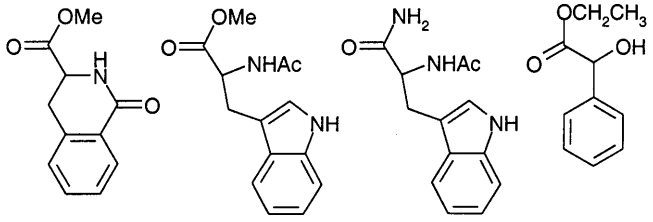

Fig. 7. Substrates used by *Ke et al.* as reported in Table 5 [56]

Table 5. Comparison of experimentally determined enantioselectivities in the chymotrypsin catalyzed hydrolyses of substrates **1**–**4** of Fig. 7 with the simulation results *in vacuo* and in aqueous solution [56]

	$\Delta\Delta G'$/ kj · mol^{-1}		
		Calculated	
Substrate	Experimental In buffer	*in vacuo*	In water
1	−20.5	−18.4	−18.8
2	>30	26.4	22.2
3	>30	33.5	36.4
4	0.4	5.0	0.4

differences in water between (*R*) and (*S*) substrates were calculated according to Eq. (6) where the first term is the difference in the bonded energy terms and the second is the difference in the *van der Waals* energy for molecular mechanics energy-minimized structures of the two intermediates. The two ΔG values in the second term of the equation are the electrostatic contributions in continuum solvent consisting of coulombic and reaction field contributions, whereas the nonpolar term is computed from the solvent-accessible surface area difference between the (*R*) and (*S*) configured enzyme-bound tetrahedral intermediates. The results were in good agreement with experimental values as reported in Table 5.

$$\Delta G_{R-S}^{\text{water}} = \Delta E_{R-S}^{\text{covalent}} + \Delta E_{R-S}^{vdW} + \Delta G_{R-S}^{\text{elec}} + \Delta G_{R-S}^{\text{nonpolar}} \tag{6}$$

This study was a considerable advance over earlier efforts, but significant improvements could still be made, especially through the use of explicit solvent and the determination of atomic point charges including the effect of the enzyme environment. This had been done in the past on ester cleavage by a β-cyclodextrin, but the first application to enzyme systems is due to *Colombo et al.* [57]. Their study focussed on the development of a deeper understanding of the enantioselectivity of the serine protease subtilisin *DMF* in with respect to the resolution of a racemic mixture of 1-phenyl-ethanol by a transesterification reaction with the acylating agent vinyl acetate. Once again, the formation of the tetrahedral intermediate is thought to be the rate determining step for catalysis (Fig. 8). Moreover, it is supposed that the structure of the transition state for the formation

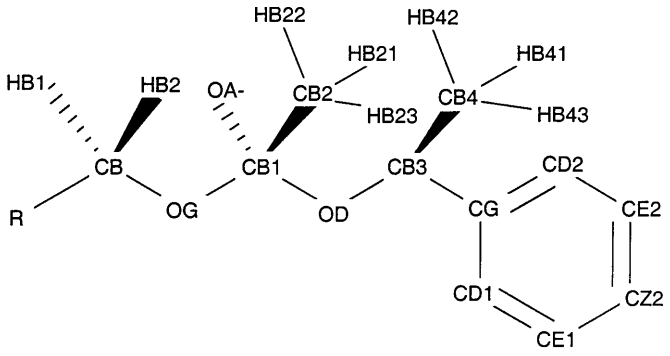

Fig. 8. Tetrahedral intermediate for the subtilisin-catalyzed transesterification of 1-phenyl ethanol with acetate (see Table 6) [57]

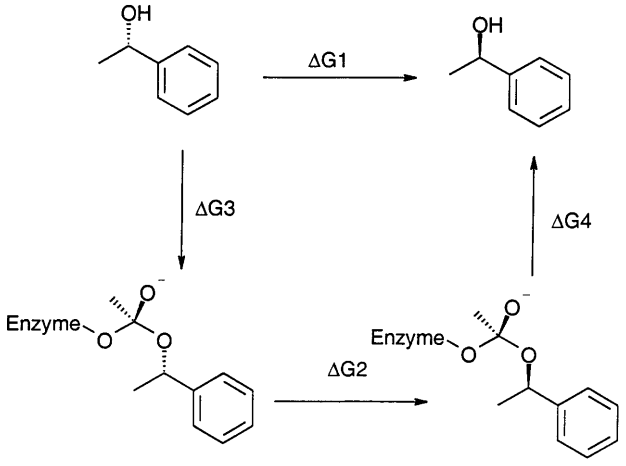

Scheme 1. Scheme for FEP calculation

of the tetrahedral intermediate closely resembles the structure of the tetrahedral intermediate itself. The behavior and the characteristics of the tetrahedral intermediates for both the (*R*) and (*S*) enantiomers were examined by means of MD and FEP simulations (Scheme 1) with an explicit representation of the organic solvent *DMF*. A critical aspect of this study was the determination of the charge distribution of the (*R*) and (*S*) tetrahedral intermediates by means of a QM/MM electrostatic potential fitting methodology. In designing the active site model, the (*R*) and (*S*) configured tetrahedral intermediates were found to have significantly different charge distributions due to the presence of the stereo-differentiating environment presented by the enzyme. In contrast, the charge distribution obtained for models of the tetrahedral intermediate in the gas-phase display similar charge distributions. From MD simulations, both steric and, more importantly, electrostatic complementarity were seen to play a role in the determination of the enantioselectivity of this enzyme reaction. Table 6 displays the differential charges on the tetrahedral intermediates for the two enantiomers and on the active site residue atoms. These point charges were then used for FEP simulations to obtain a free energy difference that was in good accordance with experiment (Table 7),

Table 6. Average ESP charges calculated for the (*R*) and (*S*) complexes of Fig. 8 [57]

	(*R*)-complex		(*S*)-complex		
Atom	Charge	Std. dev.	Charge	Std. dev.	Charge diff.
CB	−0.056	0.062	−0.029	0.063	−0.027
HB2	0.081	0.027	0.064	0.029	0.017
HB3	0.035	0.023	0.042	0.036	−0.007
OG	−0.305	0.061	−0.351	0.033	0.047
CB1	0.588	0.106	0.697	0.101	−0.108
CB2	−0.331	0.065	−0.297	0.067	−0.034
HB21	0.075	0.038	0.045	0.033	0.030
HB22	0.092	0.027	0.046	0.026	0.046
HB23	0.060	0.027	0.063	0.034	−0.003
OA-	−0.876	0.036	−0.914	0.038	0.037
OD	−0.462	0.073	−0.543	0.065	0.081
CB3	0.205	0.118	0.464	0.118	−0.258
HB3	0.045	0.059	−0.044	0.038	0.089
CB4	−0.277	0.051	−0.222	0.059	−0.054
HB41	0.052	0.022	0.042	0.027	0.010
HB42	0.065	0.024	0.033	0.031	0.032
HB43	0.095	0.027	0.050	0.017	0.045
CG	0.055	0.071	−0.047	0.075	0.103
CD1	−0.154	0.048	−0.069	0.053	−0.085
HD1	0.095	0.020	0.126	0.019	−0.031
CE1	−0.109	0.054	−0.142	0.049	0.033
HE1	0.101	0.021	0.126	0.021	0.025
CZ	−0.114	0.052	−0.116	0.042	0.001
HZ	0.097	0.020	0.093	0.023	0.004
CE2	−0.107	0.037	−0.131	0.034	0.024
HE2	0.111	0.014	0.100	0.011	0.011
CD2	−0.125	0.051	−0.139	0.045	0.014
HD2	0.117	0.013	0.099	0.015	0.018

Table 7. Calculated free energy difference for the thermodynamic cycle given in Scheme 1 [57]

Starting structure	FEP time / ps	Free energy ($\Delta\Delta G'$)/kJ · mol^{-1}
90 ps	150	6.3 ± 2.1
90 ps	450	2.5 ± 1.2
90 ps	750	5.0 ± 2.1
120 ps	450	3.3 ± 1.7
120 ps	750	5.4 ± 2.1

quantitatively supporting the accuracy of the model and suggesting that all-atom molecular simulations are capable of providing accurate qualitative and quantitative insights into enzyme catalysis in non-aqueous solvents as well as into enzyme catalysis in general.

Conclusions

In this article we have reviewed how molecular modeling techniques have been used in the last few years to shed some light on how organic solvents influence the molecular characteristics of proteins and enzymes. MD simulations on BPTI, chymotrypsin, and subtilisin made it possible to get a deeper understanding into how increased intramolecular interactions improve conformational rigidity, thus explaining the lower reactivity and the higher thermostability of enzymes in non-aqueous media. This structural information allowed to understand some peculiar aspects of the behavior of enzymes in organic solvents.

The application of thermodynamics-based models allowed the first qualitative predictions on the selectivity of many reaction types. However, only after the application of quantum mechanical/molecular mechanical methods quantitative models of actual reactivity patterns could be realistically formulated. Even though these methods are still in part approximate due to the partial application of force fields and semiempirical *Hamiltonians*, they showed that focusing the attention on the reactive region of the enzyme with QM calculations, while keeping track of the enzyme-environment influence through MD, was the right way to go. Improvements in the QM computational methods, such as the introduction of linear scaling divide-and-conquer methods [58], will certainly allow to gain a first principle understanding of the reactivity of macromolecules in any kind of environment.

Acknowledgements

We thank the CNR Target Project on Biotechnology for financial support.

References

[1] Klibanov AM, Zacks A (1984) Science **224**: 1249
[2] Klibanov AM (1986) CHEMTECH **63**: 354
[3] Zacks A, Klibanov AM (1986) J Am Chem Soc **108**: 2767
[4] West JB, Hennen WJ, Lalonde JL, Bibbs JA, Zhong Z, Meyer EF jr, Wong CH (1990) J Am Chem Soc **112**: 5313
[5] Zacks A, Klibanov AM (1985) Proc Natl Acad Sci USA **82**: 3192
[6] Kuhl P, Halling PJ, Jakubke HD (1990) Tetrahedron Lett **31**: 5213
[7] Klibanov AM (1989) TIBS **14**: 141
[8] Carrea G, Ottolina G, Riva S (1995) Trends Biotechnol **13**: 63
[9] Kazandjian RZ, Klibanov AM (1986) J Am Chem Soc **107**: 5448
[10] Ayala G, De Gomez-Poyou MT, Gomez-Poyou A, Darszon A (1986) FEBS **203**: 41
[11] Capaldi RA, Malatesta F, Darley-Usmar VM (1983) Biochim Biophys Acta **726**: 135
[12] Russel A, Klibanov AM (1988) J Biol Chem **263**: 11624
[13] Stahl M, Jeppsson-Wittstrand U, Mannson MO, Mosbach K (1991) J Am Chem Soc **113**: 9366
[14] Poole PL, Finney JL (1983) Biopolymers **22**: 255
[15] Poole PL, Finney JL (1983) Int J Macromol **5**: 308
[16] Poole PL, Finney JL (1984) Comments Mol Cell Biophys **2**: 129
[17] Careri G, Gratton E, Yang PH, Rupley JA (1980) Nature **284**: 572
[18] Hartsough DS, Merz KM (1992) J Am Chem Soc **114**: 2570
[19] McCammon JA, Gelin BR, Karplus M (1977) Nature **267**: 585

[20] Brooks CL III, Karplus M, Pettitt BM (1988) Proteins: A Theoretical Perspective of Dynamics, Structure, and Thermodynamics. Wiley, New York
[21] Frauenfelder H, Sligar SG, Wolynes PG (1991) Science **254**: 1598
[22] Zacks A, Klibanov AM (1988) J Biol Chem **263**: 3194
[23] Hartsough DS, Merz KM Jr (1993) J Am Chem Soc **115**: 6529
[24] Toba S, Hartsough DS, Merz KM Jr (1996) J Am Chem Soc **118**: 6490
[25] Yennawar NH, Yennawar HP, Farber GK (1994) Biochemistry **33**: 7326
[26] Yennawar NH, Yennawar HP, Farber GK (1995) J Am Chem Soc **117**: 577
[27] Zheng Y-J, Ornstein RL (1996) J Am Chem Soc **118**: 4175
[28] Zheng Y-J, Ornstein RL (1996) Biopolymers **38**: 791
[29] Zheng Y-J, Ornstein RL (1996) Protein Eng **9**: 485
[30] Desai UR, Klibanov AM (1995) J Am Chem Soc **117**: 3940
[31] Zheng Y-J, Ornstein RL (1996) J Am Chem Soc **118**: 11237
[32] Onsager L (1936) J Am Chem Soc **58**: 1486
[33] Hwang J-K, Warshel A (1988) Nature **334**: 270
[34] Klibanov AM (1997) Trends Biotechnol **15**: 97
[35] Tramper JVM, Vermüe MH, Beeftink HH, Von Stockar U (1992) Biocatalysis in Non-Conventional Media. Progress in Biotechnology, vol 8. Elsevier, Amsterdam
[36] Fitzpatrick PA, Steinmetz ACU, Ringe D, Klibanov AM (1993) Proc Natl Acad Sci USA **90**: 8653
[37] Fitzpatrick PA, Ringe D, Klibanov AM (1994) Biochem Biophys Res Comm **198**: 675
[38] Griebenow K, Klibanow AM (1997) Biotechnol Bioeng **54**: 210
[39] Wescott CR, Klibanov AM (1993) J Am Chem Soc **115**: 1629
[40] Wescott CR, Klibanov AM (1993) J Am Chem Soc **115**: 10362
[41] Fredenslund A, Gmelhling J, Rasmussen P (1977) Vapor-Liquid Equilibria Using UNIFAC. Elsevier, Amsterdam
[42] Ke TW, Klibanov AM (1996) J Am Chem Soc **118**: 3366
[43] Wescott CR, Klibanov AM (1996) J Am Chem Soc **118**: 10365
[44] Colombo G, Ottolina G, Carrea G, Bernardi A, Scolastico C (1998) Tetrahedron Asymm **9**: 1205
[45] Luque S, Ke T, Klibanov AM (1998) Biocatal Biotransform **16**: 233
[46] Uppenberg J, Ohrner N, Norin M, Hult K, Kleywegt GJ, Patkar S, Waagen V, Anthonsen T, Jones TA (1995) Biochemistry **34**: 16838
[47] Haeffner F, Norin T, Hult, K (1998) Biophysical J **74**: 1251
[48] Warshel A, Levitt M (1976) J Mol Biol **103**: 227
[49] Daggett V, Schröder S, Kollman P (1991) J Am Chem Soc **113**: 8926
[50] Merz KM Jr, Banci L (1996) J Am Chem Soc **118**: 10235
[51] Turner AJ, Moliner V, Williams IH (1997) J Chem Soc Chem Commun 1271
[52] Antonczack S, Monard G, Ruiz-Lopez MF, Rivail J-L (1998) J Am Chem Soc **120**: 8825
[53] Bentzien J, Muller RP, Florian J, Warshel A (1998) J Phys Chem B **102**: 2293
[54] Stanton RV, Perakyla M, Bakowies D, Kollman PA (1998) J Am Chem Soc **120**: 3448
[55] Cornell WD, Cieplak P, Bayly CI, Gould IR, Merz KM Jr, Ferguson DM, Spellmeyer D Fox T, Caldwell JW, Kollman PA (1995) J Am Chem Soc **117**: 5179
[56] Ke T, Tidor B, Klibanov AM (1998) Biotechnol Bioeng **57**: 741
[57] Colombo G, Toba S, Merz KM Jr (1999) J Am Chem Soc **121**: 3486
[58] Dixon SL, Merz KM Jr (1996) J Chem Phys **104**: 6643

Received November 18, 1999. Accepted (revised) February 8, 2000